THE ASTROPHYSICAL JOURNAL, 606:L49–L52, 2004 May 1

THE INNER ANNULAR GAP FOR PULSAR RADIATION: γ-RAY AND RADIO EMISSION

G. J. QIAO,[1,2] K. J. LEE,[2] H. G. WANG,[3] R. X. XU,[2] AND J. L. HAN[1,2]

Received 2003 December 28; accepted 2004 March 16; published 2004 April 7

ABSTRACT

The inner annular gap (IAG), a new type of inner gap whose magnetic field lines intersect the null charge surface (NCS), is proposed to explain γ-ray and radio emission from pulsars. The IAG can be an important source for high-energy particles. The particles can radiate between the NCS and the IAG. Some observational characteristics in both γ-ray and radio bands, such as the Crab-like, Vela-like, and Geminga-like γ-ray emission beams, can be reproduced by the numerical method. It is predicted that the view angle ζ should be larger than the inclination angle ($\zeta > \alpha$), otherwise the γ-ray radiation will have little possibility to be observed. Whether the IAG (or cap) is sparking (or free flow) depends on the surface binding energy of the pulsar. Instead of neutron star models, the scenario of the IAG is favorable for bare strange star models, because bare strange stars can easily satisfy the requisite condition to form an IAG for both pulsars ($\boldsymbol{\Omega} \cdot \boldsymbol{B} < 0$) and antipulsars ($\boldsymbol{\Omega} \cdot \boldsymbol{B} > 0$).

Subject headings: elementary particles — pulsars: general — radiation mechanisms: nonthermal — stars: neutron

1. INTRODUCTION

Both polar cap and outer gap models of γ-ray pulsars have been suggested to explain the high-energy emission from pulsars (Ayasli 1981; Harding 1981; Harding & Muslimov 1998; Muslimov & Harding 2003; Zhao et al. 1989; Lu & Shi 1990, 1994; Cheng et al. 1976, 1986, 2000; Ray & Benford 1981; Hirotani 2000; Romani 1996, 2002). Here, we propose a new scenario of the inner annular gap (IAG) outside the conventional inner gap. The IAG is defined by magnetic field lines that intersect the null charge surface (NCS; see Fig. 1). As we know, at any point on the NCS the direction of the local magnetic field is perpendicular to the rotation axis. So if the radiation region is located near the NCS (either inside or outside), the pulsar can easily produce a very wide pulse profile (Qiao et al. 2003a). This wide profile will match the observed γ-ray pulse profiles rather well. Some authors (Qiao et al. 2003a, 2003b; Dyks & Rudak 2003) suggest that if the emission region is located inside the NCS, it would help us to understand the γ-ray emission. Here we suggest that the particles flowing out from the IAG could be reaccelerated and radiate γ-rays inside the NCS, and this model could account for the γ-ray and radio emission occurring at the same time. In § 2 the basic ideas for the IAG are presented. In § 3 we show how γ-ray and radio emissions can be produced. Conclusions and a brief discussion are given in § 4.

2. DETAILS OF THE IAG

Figure 1 illustrates the magnetosphere of an oblique rotator with a dipolar magnetic field configuration. The magnetic field line "c" is the critical field line, which intersects the NCS at the light cylinder. The radius of the polar cap region defined by the critical field lines in an aligned rotator is $r_{\rm in} = 0.74\Omega^{0.5}R^{1.5}c^{0.5}$ (Ruderman & Sutherland 1975, hereafter RS). Here R (cm) and Ω are the radius and the angular velocity of the star, respectively, and c is the light speed. The cap radius at the foot of the last open field line is $r_p = \Omega^{0.5}R^{1.5}c^{0.5}$. There is an annulus between r_p and $r_{\rm in}$.

Two kinds of inner vacuum gaps above the polar cap may be formed in some circumstances: the conventional inner core gap (ICG) above the central part of the polar cap and the IAG above the annular part of the polar cap. If the width of the IAG is large enough, the potential drop in the IAG would be high enough so that sparking will be able to take place there. The sparking leads to pair production and generates the secondary pairs, which are accelerated out of the IAG.

For neutron stars, the binding energy of positive particles could be high enough only under some special conditions (Gil & Mitra 2001; Gil & Melikidze 2002) to lead to the formation of an inner vacuum gap. Only one of the inner vacuum gaps can form in this case: an IAG for a pulsar ($\boldsymbol{\Omega} \cdot \boldsymbol{B} < 0$) or an ICG for an antipulsar ($\boldsymbol{\Omega} \cdot \boldsymbol{B} > 0$). However, the physical condition changes for bare strange stars. The IAG and ICG can form in this case, whether the star is a pulsar or an antipulsar, since the binding energy is roughly infinite (Xu et al. 1999, 2001). The width of the IAG is a function of the inclination angle α, as Figure 2 shows. In the dipolar configuration, the field lines are traced to obtain the shapes of the IAG and ICG. When α increases, the width of the annular gap between the magnetic axis and the equator (region A) becomes wider, and a higher potential drop can be obtained to produce sparks. At the same time, the width of the IAG between the rotational and magnetic axes (region B) becomes narrow and has little chance to form sparks.

Pair cascades can develop in the IAG, and the secondary pairs are produced in an intrinsically nonstationary mode, just as like what occurs in an RS-type gap. The secondary pairs are generated as small bundles. In the RS gap model, these bundles of nonneutral plasma will no longer endure acceleration out of the gap. Does this still hold true for the IAG scenario? Probably not; we note that several factors may lead to reacceleration out of the IAG.

First, because of field line curvature, the net charge density will depart from the local Goldreich & Julian (1969, hereafter GJ) charge density when particles move along the magnetic field lines, which induces parallel electric fields. This effect is especially strong in the magnetic tube rooted in the IAG, because the GJ charge density varies more sharply than on other

[1] National Astronomical Observatories, Chinese Academy of Sciences, A20 Datun Road, Chaoyang Beijing 100012, China.
[2] Department of Astronomy, Peking University, 5 Haidian Lu, Beijing 100871, China.
[3] Center for Astrophysics, Guangzhou University, Guangzhou 510400, China.

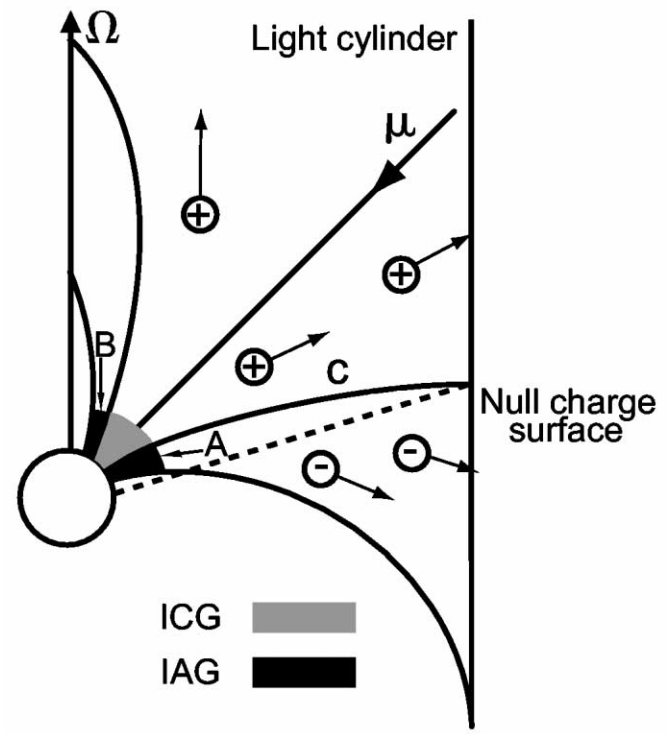

FIG. 1.—IAG, ICG, and NCS of an oblique rotator. If the center star is a strange star, both the IAG and the ICG can work. For neutron stars, only one inner gap can be formed.

open field lines, and even the local changes from one sign to the opposite sign when moving across the NCS. Second, it is normally suggested that the self-consistent adjustment of the net charge of nonneutral plasma is able to screen the parallel electric fields. However, when charged particles are moving at relativistic velocities and are bunched into bundles, one has to calculate the electric field by consulting the Liénard-Wiechert potential rather than the Coulomb potential. It is known that for a relativistic charge particle (with a Lorentz factor γ), the electric field on the moving direction is reduced by a factor of $1/\gamma^2$; the screen electric field generated by the secondary pairs should also be reduced by a factor of $1/\gamma^2$, which may be neglected to compare with the reacceleration electric field (K. J. Lee et al. 2004, in preparation).

In this Letter, we simply assume that the secondaries are reaccelerated and radiate photons in the region between the NCS and the IAG. We then aim to find whether it is feasible to account for γ-ray and radio properties of pulsar emission. The next section is an endeavor to reproduce the observational properties at γ-ray and radio bands based on the assumption.

3. GAMMA-RAY AND RADIO EMISSION FROM PULSARS

Basic picture for γ-ray emission.—As it is assumed that γ-ray emission can be produced between the NCS and the IAG, wide pulse profiles can also be produced there. To simulate the observations, geometry is important. The radiation geometry is shown in Figures 1 and 3, where ϕ is the azimuthal angle around the magnetic axis, α is its inclination angle, and θ is the angle between the magnetic axis and the radiation location

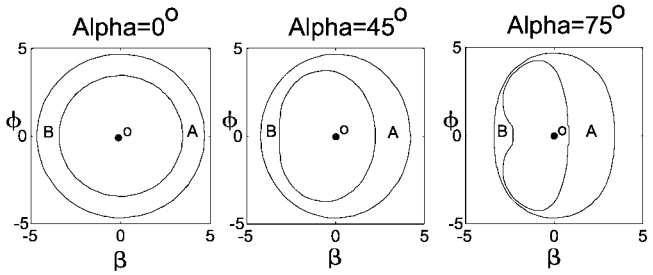

FIG. 2.—Shape of the IAG and the ICG for different inclination angles α. A dipole magnetic field configuration is used in the calculations.

r. The angle between the magnetic axis and the NCS, θ_N, has the form of

$$\theta_N(\phi) = \frac{1}{2}\arccos\frac{\chi\cos\phi\sin\alpha - \cos^2\alpha}{3(\cos^2\alpha + \cos^2\phi\sin^2\alpha)}, \qquad (1)$$

where $\chi = (8\cos^2\alpha + 9\cos^2\phi\sin^2\alpha)^{0.5}$. The distance from the center of the star to the intersection of the last open magnetic field lines and the NCS is denoted by $r_N(\phi)$. For a dipole field configuration, $r_N(\phi) = R_0(\phi)\sin^2[\theta_N(\phi)]$, where $R_0(\phi)$ is the maximum radius of the last open field line. The distance from the star center to the emission point is $r(\phi) = \kappa[\lambda r_N(\phi) + (1-\lambda)r_N(0)]$, where λ and κ are the two parameters used to indicate the radiation location. For simplicity, we take λ and κ as 0.8 in our calculations. The physical meaning of $\kappa = 0.8$ is that the radiation positions are located near the NCS and the distance of the radiation location is roughly proportional

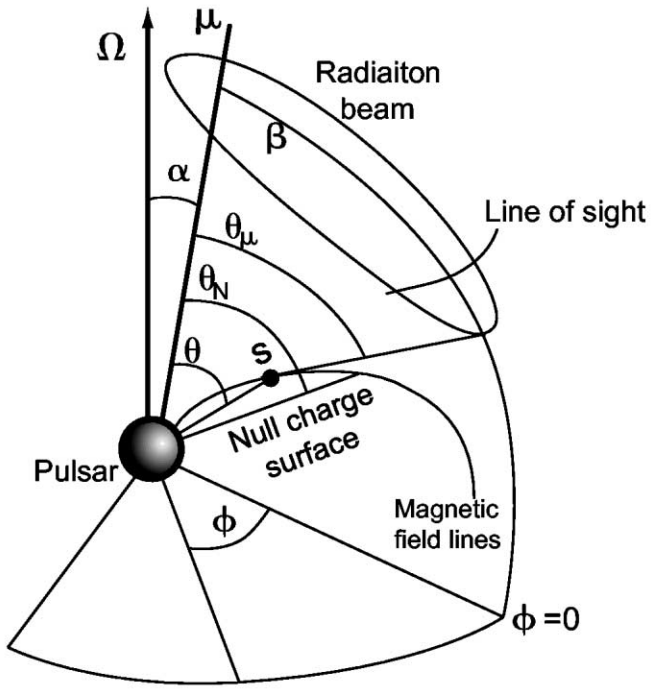

FIG. 3.—Radiation geometry of a pulsar. Here ϕ, ζ, and α are the azimuthal angle with respect to the magnetic axis, the viewing angle, and the inclination angle, respectively, and θ, θ_μ, and θ_N denote the angle between the magnetic axis and the radiation source S, the radiation direction, and the null charge surface, respectively. Owing to the aberration effect, as well as because at different radiation positions the NCS plays a different role, the radiation beam is asymmetric.

to the distance of the NCS. Here $\lambda = 0.8$ means that the distance of the radiation location is not exactly proportional to that of the NCS and needs correction, when the NCS is located far from the star.

For the last open field line, the angle between the radiation direction and the magnetic axis, θ_μ, is also a function of the azimuthal angle ϕ, which reads

$$\theta\mu = \arctan\frac{3\sin(2\theta)}{1 + 3\cos(2\theta)}, \quad (2)$$

where $\theta(\phi) = \arcsin[r(\phi)/R_0(\phi)]^{0.5}$. The aberration correction is performed on the θ_μ by numerical procedures. Pulse phase separations can be figured out by direct but lengthy mathematics, which involves the impact angle ξ ($\xi = \zeta - \alpha$). The calculated pulse profiles and parameters are given in Figure 4. The width and height of each component in the mean pulse profile are input-free parameters. But phase separation is firmly related to the parameters α, ξ, λ, and κ. The physical considerations for the parameters are as follows.

Physical and geometrical limitations of γ-ray emission regions.—The Lorentz factor of the secondary particles out of the inner gap can reach 10^3 (Zhang et al. 1997). When the secondary particles move out from the IAG, they lose their energy through various mechanisms simultaneously, and inverse Compton scattering plays an important role (Xia et al. 1985; Dyks & Rudak 2000; Zhang & Harding 2000). Magnetic inverse Compton scattering is also an important source of hard γ-ray photons (Sturner et al. 1995). This means that the hard γ-ray radiation could be produced just out of the gap. However, the position where such γ-rays can escape is limited by the γ-ray attenuation effect in the strong magnetic fields.

A spectral cutoff of γ-ray pulsars above 10–100 GeV (Kildea 2003) presents a lower limit of the distance from the emission location from the stellar center. Detailed calculation shows that the 100 GeV photons can only escape from the distance at least above $20R$ for both the Crab (surface magnetic strength B_0 is 3.7×10^{12} G) and the Vela ($B_0 = 3.3 \times 10^{12}$ G) pulsars. We obtain $\kappa > 0.5$ and 0.2, respectively, for the Crab and Vela pulsars in the model.

The calculation indicates that the parameters λ and κ will affect the phase separation between the two peaks of the γ-ray light curve. For Crab and Vela (see Fig. 4), we find $\kappa \in (0.8, 0.99)$ and $\lambda \in (0.65, 0.85)$ for Crab and $\kappa \in (0.65, 0.83)$ and $\lambda \in (0.77, 0.99)$ for Vela, for a 10% change in the phase separation for the two peaks. The values of κ and λ indicate that the main radiation region is confined near the NCS.

Radio emission.—The inverse Compton scattering model (Qiao & Lin 1998; Xu et al. 2000; Qiao et al. 2001, 2002) is involved in our IAG model to account for the radio emission. The secondary pairs streaming out from the polar cap cascade with a typical energy $\gamma = (1 - \beta^2)^{-0.5} \sim 10^3$ and will scatter the low-frequency waves produced by the sparking, and the upscattered frequency reads $\nu \simeq 2\gamma^2\nu_0(1 - \beta\cos\theta_i)$ (for $B \ll B_q = 4.414 \times 10^{13}$ G), where θ_i is the incident angle (the angle between the moving direction of the particle and the incoming photon). The differences between the observed radio and γ-ray pulse profiles are very significant.

Figure 4 shows the calculated Crab-like, Vela-like, and Geminga-like light curve for both the radio and the γ-ray band under reasonable parameters. The observed pulse profiles in γ-ray and radio bands are reproduced for seven pulsars: the Crab, PSR B1509−58, the Vela, PSR B1706−44, PSR B1951+32, the Geminga, and PSR B1055−52 (Qiao et al. 2003a, 2003b).

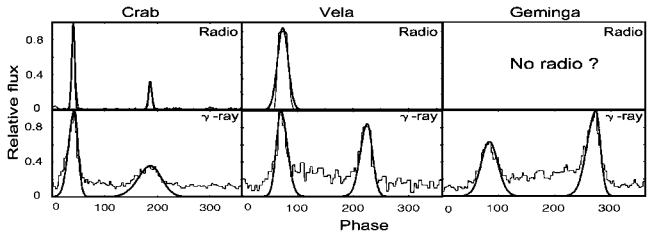

FIG. 4.—Theoretical and observed Crab-like, Vela-like, and Geminga-like light curves at both radio and γ-ray bands. The γ-ray and radio data are derived from Thompson (2003) and the European Pulsar Network Data Archive, respectively. The parameters listed in the figure are just for reference. If phase separation is determined with 10% error, we found that $0.8 < \kappa < 0.99$, $0.65 < \lambda < 0.85$, $36° < \alpha < 49°$, $39° < \zeta < 57°$ for Crab and $0.65 < \kappa < 0.83$, $0.77 < \lambda < 0.99$, $33° < \alpha < 44°$, $51° < \zeta < 61°$ for Vela. We do not give parameters for the Geminga light curve; the parameters cannot be gotten only from the γ-ray light curve.

4. CONCLUSIONS AND DISCUSSIONS

We emphasize here that the IAG and the NCS play an important role in pulsar γ-ray radiation; at least the IAG can be a source of high-energy particles for pulsar emission. If the radiation region is located near the NCS, many radio and γ-ray observational facts can be easily understood. The large phase separation of γ-ray pulse profiles reveals that the γ-ray radiation region should be located near the NCS. The geometry calculation partly supports this radiation location.

It is indicated from the calculation above and from the condition of γ-ray pulsars that we observed that the view angle ζ should be larger than the inclination angle, i.e., $\beta > 0$. This is because the part of the IAG between the magnetic axis and the equator is wider, so that it gains a higher potential drop when the inclination angle becomes larger.

The luminosity of γ-ray pulsars in the IAG model depends on the maximum potential drop across the gap, $\Delta V = 0.5\Omega B r_p^2 c^{-1}$. For a given Lorentz factor we find that the γ-ray luminosity is proportional to $P^{0.5}P^{-1.5}$, which is in agreement with observations.

Our IAG scenario is intrinsically different from the free-flowing type of polar cap model. How does the IAG interact with the outer gap? Are pulsars bare strange stars or a special kind of neutron star (Gil & Melikidze 2002)? Does the radiation come from the reaccelerated nonstationary pair flow or free flow? All of these questions need to be investigated further. The details of the IAG model, such as the reacceleration and radiation processes, γ-ray luminosity, spectral behaviors, emission beam properties, and so on, will be discussed in separate papers.

We are very grateful to Professor R. N. Manchester and B. Zhang for their valuable suggestions. The anonymous referee is sincerely acknowledged. This work is supported by the NSF of China (10373002, 10273001).

REFERENCES

Ayasli, S. 1981, ApJ, 249, 698
Cheng, A., Ruderman, M., & Sutherland, P. 1976, ApJ, 203, 209
Cheng, K. S., Ho, C., & Ruderman, M. A. 1986, ApJ, 300, 500
Cheng, K. S., Ruderman, M. A., & Zhang, L. 2000, ApJ, 537, 964
Dyks, J., & Rudak, B. 2000, A&A, 360, 263
———. 2003, ApJ, 598, 1201
Gil, J., & Melikidze, G. I. 2002, ApJ, 577, 909
Gil, J., & Mitra, D. 2001, ApJ, 550, 383
Goldreich, P., & Julian, W. H. 1969, ApJ, 157, 869 (GJ)
Harding, A. K. 1981, ApJ, 245, 267
Harding, A. K., & Muslimov, A. G. 1998, ApJ, 508, 328
Hirotani, K. 2000, PASJ, 52, 645
Kildea, J. 2003, preprint (astro-ph/0305580)
Lu, T., & Shi, T. 1990, A&A, 231, L7
Muslimov, A. G., & Harding, A. K. 2003, ApJ, 588, 430
Qiao, G. J., Lee, K. J., Wang, H. G., & Xu, R. X. 2003a, in IAU Symp. 214, High Energy Processes and Phenomena in Astrophysics, ed. X. D. Li, V. Trimble, & Z. R. Wang (San Francisco: ASP), 167
———. 2003b, in ASP Conf. Ser. 302, Radio Pulsars, ed. M. Bailes, D. J. Nice, & S. E. Thorsett (San Francisco: ASP), 83
Qiao, G. J., & Lin, W. P. 1998, A&A, 333, 172
Qiao, G. J., Liu, J. F., Zhang, B., & Han, J. L. 2001, A&A, 377, 964
Qiao, G. J., Wang, X. D., Wang, H. G., & Xu, R. X. 2002, Chinese J. Astron. Astrophys., 2, 361
Ray, A., & Benford, G. 1981, Phys. Rev. D, 23, 2142
Romani, R. W. 1996, ApJ, 470, 469
———. 2002, in ASP Conf. Ser. 302, Radio Pulsars, ed. M. Bailes, D. J. Nice, & S. E. Thorsett (San Francisco: ASP), 331
Ruderman, A. M., & Sutherland, P. G. 1975, ApJ, 196, 51 (RS)
Sturner, S. J., Dermer, C. D., & Michel, F. C. 1995, ApJ, 445, 736
Thompson, D. J. 2003, in IAU Symp. 218, Young Neutron Stars and Their Environment, ed. F. Camilo & B. M. Gaensler (San Francisco: ASP), 223
Xia, X. Y., Qiao, G. J., Wu, X. J., & Hou, Y. Q. 1985, A&A, 152, 93
Xu, R. X., Liu, J. F., Han, J. L., & Qiao, G. J. 2000, ApJ, 535, 354
Xu, R. X., Qiao, G. J., & Zhang, B. 1999, ApJ, 522, L109
Xu, R. X., Zhang, B., & Qiao, G. J. 2001, Astropart. Phys., 15, 101
Zhang, B., & Harding, A. K. 2000, ApJ, 532, 1150
Zhang, B., Qiao, G. J., & Han, J. L. 1997, ApJ, 491, 891
Zhao, Y. H., Lu, T., Huang, K. L., Lu, J. L., & Peng, Q. H. 1989, A&A, 223, 147